Analyst

COMMUNICATION

View Article Online
View Journal | View Issue

CrossMark click for updates

Cite this: *Analyst*, 2015, **140**, 1421

Received 25th November 2014,
Accepted 8th January 2015

DOI: 10.1039/c4an02169j

www.rsc.org/analyst

Micromotors to capture and destroy anthrax simulant spores†

Jahir Orozco, Guoqing Pan, Sirilak Sattayasamitsathit, Michael Galarnyk and Joseph Wang*

Towards addressing the need for detecting and eliminating biothreats, we describe a micromotor-based approach for screening, capturing, isolating and destroying anthrax simulant spores in a simple and rapid manner with minimal sample processing. The *B. globilli* antibody-functionalized micromotors can recognize, capture and transport *B. globigii* spores in environmental matrices, while showing non-interactions with excess of non-target bacteria. Efficient destruction of the anthrax simulant spores is demonstrated *via* the micromotor-induced mixing of a mild oxidizing solution. The new micromotor-based approach paves a way to dynamic multifunctional systems that rapidly recognize, isolate, capture and destroy biological threats.

Introduction

Growing concerns regarding biological weapon agents (BWA) have led to urgent needs for rapid, sensitive and cost-effective detection and destruction methods.[1a,b] Currently available methods for detection include PCR-, immuno- and array-based sensors and biosensors.[1c] Although sensitive and specific, some of them are costly or not amenable to high-throughput analyses and their applicability to real samples still represents a challenge.

Particularly important and challenging is the detection and elimination of *Bacilus anthracis*, a rod-shaped, Gram-positive, saprophytic bacterium that causes anthrax.[2a] Soil, vegetation and water are the most common habitats of anthracis. These bacteria can form spores, which are very resistant to environmental changes and can even remain viable for decades. The use of mono and polyclonal antibodies for the detection (and quantification) of *Bacillus anthracis* in different formats has been patented[2a] and broadly explored,[2a–e] including immuno chromatographic assays that use colloidal gold to visualize the reaction in environmental samples.[2b] Regarding decontamination responses, common antimicrobial agents including bleach, chlorine dioxide, hydrogen peroxide, and paraformaldehyde have been shown to be relevant for the inactivation of *Bacillus anthracis* cells.[3] However, due to the highly protective coat, spores are much more resistant than their vegetative cell counterparts to many chemical disinfectants and physical treatments so that effective decontamination protocols are highly required. With advances in nanotechnology, several natural and engineered nanomaterials have shown strong antimicrobial properties that are promising for environmental applications. For example, carbon nanotubes have led to effective inactivation of spores by perturbing their coating and facilitating accessibility of oxidizing agents.[3] Such nanomaterials have helped to reduce resistance of spores to the oxidizing chemical sporicidal, and to achieve enhanced inactivation efficiency, while reducing the potential risk of excessive chemicals to environmental and biological matrices.

Self-propelled tubular micromotors,[4–7] powered by chemical fuels (*e.g.*, hydrogen peroxide), have recently attracted considerable attention towards diverse biomedical[8–11] and environmental[12–14] applications owing to their attractive cargo-towing and solution-mixing capabilities. The efficient motor-induced fluid mixing of such tubular microengines has shown to be extremely effective in accelerating both target-receptor recognition reactions[8–10] and detoxification processes.[12–14] Micromotors have also been used for enhanced protein detection in connection with new lab-on-chip[8] and microarray[9] immunoassays.

This article demonstrates the first example of a micromotor-based approach for dramatically enhancing the isolation and destruction of spores of *Bacillus globigii*, a *Bacillus anthracis* simulant. The new approach relies on the ability of functional self-propelled micromotors to screen for, detecting and degrading rapidly the biothreat agent in a simple and efficient manner and with minimal sample processing. The new assay comprises anti *B. globilli* antibody-functionalized micromotors able to navigate in a contaminated solution to recognize, capture, transport and isolate single and multiple *B. globigii*

Department of Nanoengineering, University of California, San Diego, La Jolla, California 92093, USA. E-mail: josephwang@eng.ucsd.edu

†Electronic supplementary information (ESI) available. See DOI: 10.1039/c4an02169j

spores. Effective discrimination against excess of non-target *Staphylococcus aureus* and *Escherichia coli* species is demonstrated, along with successful operation in common environments where spores can be found (*e.g.*, lake or tap water). Subsequently, accelerated damage (destruction) of anthrax simulant spores is illustrated through greatly enhanced mixing of mild quiescent oxidizing solutions imparted by unfunctionalized micromotors. Similarly, the micromotor-induced mixing accelerates also the immunoreactions while the similar size of both micromotors and spores allows for a convenient label-free visualization of the presence of the threat. The new micromotor-strategy thus represents an effective approach for detecting the presence of biological threats and mitigating their potential harm.

Materials and methods

Synthesis of multilayer micromotors

The multilayer microtubular motors were prepared using a common template directed electrodeposition protocol.[1] A cyclopore polycarbonate membrane, containing 5 mm maximum diameter conical-shaped micropores (Catalog no. 7060-2513; Whatman, Maidstone, UK), was employed as a template. A 75 nm gold film was first sputtered on one side of the porous membrane to serve as a working electrode using a Denton Discovery 18. Sputtering was performed at room temperature under vacuum of 5×10^{-6} Torr, DC power 200 W and Ar was flowed at 3.1 mT. Rotation speed was 65 rpm along with a sputtering time of 90 s. A Pt wire and an Ag/AgCl with 3 M KCl were used as counter and reference electrodes, respectively. The membrane was then assembled in a plating cell with an aluminum foil serving as contact for the working electrode. To facilitate the antibody immobilization, the outermost polymeric layer was synthesized by heterogeneous co-electropolymerization of COOH-Py and EDOT from an electroplating solution containing a mixture of the monomers. The polypyrrole (PPy)-COOH/PEDOT microtubes were electropolymerized for a total charge of 0.3 C at +0.80 V from a plating solution containing 12 and 3 mM EDOT and PPy-COOH monomer, respectively, and 100 mM SDS and 7.5 mM KNO_3, all of them were prepared from Sigma-Aldrich reagents. Then, the metallic layers were deposited from a Pt and Ni solutions with three washings of the electrochemical cell in between processes. A commercial platinum solution was employed (Platinum RTP; Technic Inc., Anaheim, CA) and the nickel solution was prepared by 11 g l^{-1} $NiCl_2{\cdot}6H_2O$, 300 g l^{-1} $Ni(H_2NSO_3)_2{\cdot}4H_2O$, 30 g l^{-1} H_3BO_3 and 0.0488 g l^{-1} SDS. The intermediate Ni layer was deposited amperometrically at −1.2 V for 3.5 C to achieve the magnetic properties that allows the micromotor guidance by properly orienting the magnetic field created by a simple neodymium magnet. The catalytic inner Pt layer was deposited galvanostatically at −2 mA for 1300 s. To release the microengines from the template, the sputtered gold layer was completely removed by mechanical hand polishing with 3–4 μm alumina slurry. The membrane was then dissolved in methylene chloride for 10 min to completely release the microtubes. Finally, the released microtubes were washed repeatedly with methylene chloride, followed by ethanol and ultrapure water (18.2 MΩcm), two times each, and collected by centrifugation at 7000 rpm for 3 min after each wash.

Micromotors functionalization

The standard chemistry of 1-ethyl-3-(3-dimethylaminopropyl) carbodiimide (EDC)/*N*-hydroxysuccinimide (NHS) (from Sigma) was used to activate the carboxyl-terminal groups from the polymer for conjugation with goat anti-*Bacillus globigii* IgG (from Tetracore, TC-7014-YYY). For this purpose, micromotors were treated with 100 μl of a 0.025 M MES buffer solution pH 6.5, containing 20 mM EDC and 40 mM NHS for 30 min, washed with MES buffer for 3 min and incubated with the antibody (180 μg ml^{-1}) in PBS (1×) pH 7.2 for 2 h. The excess antibody was washed away in PBS buffer (1×) pH 7.2, containing 0.05% Tween-20. The remaining amine reactive-esters from the activated carboxylic groups were blocked with 1 M ethanolamine solution, pH 8.5, for 20 min and BSA 1% for 1 hour with a washing step in between in PBS (1×) 0.05% Tween-20 pH 7.2. In all the washing steps, the micromotors were centrifuged at 7000 rpm for 3 min. All functionalization experiments were carried out under shaking at room temperature.

Equipment

Template electrochemical deposition of microtubes was carried out with a CHI 661D potentiostat (CH Instruments, Austin, TX). An inverted optical microscope (Nikon Eclipse Instrument Inc., Ti-S/L100), coupled with a 20× and 40× objectives, along with a Hamamatsu digital camera C11440 and a NIS-Elements AR 3.2 software, were used for capturing movies at a frame rate of 10 frames per second. Two blue excitation B-2A filters: one with a 515 nm cut-on barrier filter from Nikon and the other one with an AT535/40m, 590–650 nm barrier filter, from Chroma Technology Corporation were used to visualize the stained intact and damaged cells, respectively.

Capture of spores by antibody-functionalized micromotors

B. globigii spores (preparation from Tetracore T241002-01. 6.7 mg ml^{-1}, 3.8×10^9 CFU ml^{-1}) were diluted in PBS pH 7.2 to get a working solution of 3.8×10^8 CFU ml^{-1}. Equal volumes (2 μl) of spores, micromotors, surfactants and fuels (prepared in 1× PBS buffer pH 7.4) were placed in a glass slide to get a final concentration of 1X = 9.5×10^7 CFU ml^{-1} spores, 8×10^3 micromotors (1×10^6 micromotors per ml), 5% NaCh and 3% H_2O_2. Tracking of the micromotors were done using the inverted optical microscope. Similar size of the micromotors and the spores allowed a label-free visualization of the capturing event. Control experiments were performed by using either unmodified micromotors navigating in 5× spores solution or anti-*B. globigii* antibody-modified micromotors navigating in a 10× *Staphylococcus aureus* or 1× *Escherichia coli* bacteria solutions, prepared in PBS buffer pH 7.4, keeping the fuel and surfactant levels constant. Experiments in real samples were

performed with tap water and lake water diluted 1 : 1 (or 3 : 1) in PBS buffer pH 7.4. Tap water and lake water samples were collected from the public supply system and Wohlford Lake, San Diego County, California, respectively. For the samples, anti-*B.globigii* antibody-modified micromotors navigating in a 1× spore solution were used as positive controls in comparison with unmodified micromotors navigating in samples with spore concentrations of 1× (lake sample), 2× or even 5× (tap water sample).

Destruction of *B. globigii* spores

B. globigii spores (solid biomaterial with 3.52×10^{12} cell g^{-1}, from The U.S. Army-Dugway Proving Ground) were weighed and diluted in deionized water to obtain 3.52×10^{10} CFU ml^{-1}. A cleaning step was necessary to eliminate some silica added to the cells to increase flowability (for dispersion purposes) by centrifuging the spores at low speed of 1000 rpm for 1 min and separating the supernatant (the spores) from the precipitate (the silica). Spores were centrifuged again and some micromotors, aqueous H_2O_2 and NaCh solutions were added to the pellet to obtain 15 ml final volume with concentrations of 8×10^5, 1.5 and 2%, respectively. Control experiments were performed only in water, or in water containing only H_2O_2 or only micromotors, by keeping constant the other variables. 200 μl aliquots of the reaction mix were placed in triplicate every 15 min (up to 60 min) in Eppendorf tubes containing 500 μl of 0.66 M $NaSO_3$ to stop the reaction. The mixture was centrifuged at 10 000 rpm for 10 min and the pellet was resuspended in 100 μl of a 1 : 1 mixture of Syto-9 dye/propidium iodide dye solutions, based on the instructions from the L13152LIVE/DEAD® BacLight bacterial viability kit. Eppendorf tubes were covered with aluminum foil and gently shaken for 15 min, afterwards they were centrifuged at 10 000 rpm for 10 min and the pellet was resuspended in 25 μl of water. Images of 1 μl drops were taken and the number of intact and damaged cells was estimated by using the ImageJ program. The number of intact cells was estimated by subtracting the number of damaged cells (stained with propidium iodide) from the total number of cells (stained with Syto-9) and normalized with respect to the total number of cells counted for each specific time.

Results and discussion

The micromotor-based approach has the multitasking ability to screen for the detection and destruction of biothreat agents rapidly in a simple fashion and with minimal sample processing. The immunoassay consists of anti-*B. globigii* antibody-functionalized micromotors that navigate in a contaminated solution and are able to recognize, capture and transport single and multiple *B. globigii* spores. The functionalized micromotors can thus reveal the identity of the biothreat; their similar micrometer size to the size of the spores allows a label-free visualization of the captured target. Fig. 1A illustrates the micromotor-based immunoassay with the anti-*B. globigii* antibody-functionalized micromotors capturing and transporting *B. globigii* spores towards an isolated compartment from where an efficient micromotor-accelerated oxidative destruction task can be carried out (Fig. 1B). Here, microtube engines with a new composition, including carboxy polypyrrole, *i.e.*, (COOH-PPy):PEDOT/Ni/Pt multilayers, were prepared using our template-based electrodeposition method.[5] The exposed carboxy moieties of the new COOH-PPy/metal tubular motors can facilitate covalent attachment of the antibodies. Even though EDOT derivatives have enhanced electrochemical stability and ordered structure, compared to those based on PPy,[15] the new microtubular structures have similar morphological and structural properties as earlier PEDOT-based micromotors.[8] The Py-COOH monomer thus represents a useful alternative for fabricating tubular micromotors containing carboxy moieties. Amino moieties of the antibodies can thus be covalently attached to the carboxylic groups of the outermost motor surface *via* a common carbodiimide (EDC)/*N*-hydroxysuccinimide (NHS) reaction.[8] The intermediate Ni layer provides the motor with a magnetic guidance capability while the inner catalytic Pt layer is used for the oxidation of the H_2O_2 fuel and generating the O_2 bubbles thrust essential for the self-propulsion (see ESI Video 1†). Fig. 1A illustrates the navigation of the functionalized micromotors in a buffered solution contaminated with *B. globigii* spores (a), a functionalized micromotor transporting two spores (b), as well as carrying multiple spores (c) through interactions between the surface-confined antibody receptor and proteins expressed in the spore cell wall. It is important to note that 90% of the resulting 20 μm-long and 5 μm diameter unfunctionalized COOH-PPy-EDOT micromotors are able to swim in aqueous solutions at a speed of ~250 μm s^{-1} (~12.5 body length s^{-1}) in the presence of 3% H_2O_2, which is ~1.6-fold slower compared to the ~8μm-long and 2 μm diameter unfunctionalized EDOT-COOH-EDOT microtubes (400 μm s^{-1}). Furthermore, 75% of the micromotors functionalized with anti-*B. globigii* antibodies still navigate at ~125 μm s^{-1}, which is sufficient to capture and transport the spores, as shown in Fig. 1A(b and c). The speed of the

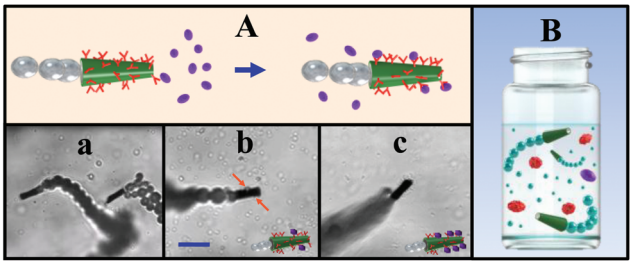

Fig. 1 (A) Schematic of the functionalized micromotors capturing and transporting *B. globigii* spores for their further destruction (B). Time-lapse images illustrating the magnetically-guided propulsion of anti-*B. globigii* antibody-PPy-COOH-PEDOT/Ni/Pt micromotors in a spore-containing aqueous solution (a) and functionalized micromotors transporting two target (b) and multiple target (c) spores. (B) Sketch of micromotors swimming in a spore-containing solution for the accelerated destruction of the spores. Spores, highlighted with an arrow. Scale bar, 20 μm.

unmodified micromotors remains constant even after storage in deionized water for several weeks. The speed was reduced only slightly by decreasing the concentration of fuel, *e.g.* micromotors moved at 124 μm s^{-1} in 1% H_2O_2 after one week of storage in water. Overall, the results of Fig. 1A demonstrate the attractive propulsion and navigation behavior of the functionalized micromotors towards the bio-separation of *B. globigii* spores. As will be discussed later, the captured spores could be destroyed by transfer into a proper destruction compartment.

To demonstrate the capability of the anti-*B. globigii* functionalized micromotors to alert about the presence of biological threats, we used the innocuous *B. globigii* spores to simulate the highly dangerous anthracis spores. Such use of innocuous microorganisms is a valuable method to emulate hazardous organisms and obviate potential risks, towards the manipulation and detection of biological threats.[16] Various control experiments demonstrated the high selectivity of the method. Fig. 2A(a–c) and ESI Video 2 show an anti-*B. globigii* antibodies-functionalized micromotor approaching (a), contacting (b) and carrying (c) a *B. globigii* target spore, in a PBS solution containing the H_2O_2 fuel. The results demonstrate that receptor-functionalized micromotors can rapidly interact with spores, leading to 'on the fly' instantaneous binding event that can be readily visualized toward a simple label-free identification of a potential biological threat. The capture efficiency of the spores depends upon the number of modified micromotors and navigation time in the contaminated solution. The micromotor approach has the added advantage of obviating washing steps common to standard immunoassays and offers a significant kinetic advantage associated with the micromotor movement, as demonstrated in other motor-based bioassays.[8–10] Fig. 2B and corresponding ESI Video 3† illustrate the high selectivity of the method using excess of nontarget agents (b, c) as well as unmodified motors (a). These show unfunctionalized micromotors contacting and bypassing the spores present at 5-fold concentration excess (a), and modified micromotor bypassing both *S. aureus cells* at 10-fold excess (b) and *E. coli* at same concentration (c), under similar conditions. Therefore, from the above discussion, it can be concluded that the specificity of the present micromotor approach is almost 100% in the presence of 10-fold excess concentration of *E. coli* and *S. aureus*.

The major interest of *anthracis* bacteria is associated with the fact that their highly resistant spores can remain viable in soil, vegetation and natural water even for decades, thereby constituting a major environmental issue and/or health threat. Accordingly, we examined the ability of the new immunomodified micromotors to capture anthrax simulant spores in relevant environmental media. Fig. 3A and B and ESI Videos 4 and 5† show the anti-*B. globigii* antibodies-functionalized micromotors capturing spores while navigating in a 1 : 1 diluted tap (Aa) or lake water (Ba) real samples. In contrast, no such binding is observed using the respective unmodified micromotors and real samples containing 2- fold and 5-fold excess of spores under similar conditions (Fig. 3Ab and Bb, respectively). While the antibodies-functionalized microengines navigate at ~60.6 μm s^{-1} in the PBS (pH 7.4) buffer solution, they propel at 34.2 and 32.3 μm s^{-1} in tap water and lake water samples, respectively. Such speeds are sufficient for the instantaneous capture of the spores demonstrating the feasibility of using the antibody-modified micromotors for identifying the presence of biothreats in real samples. It is important to note that speeds after and before spore capturing did not have statistically significant differences ($p < 0.05$) unlike a recent work that showed differences on the micromotors speed after and before capturing microparticle-tagged proteins.[10] Capture of multiple cells was also achieved by the antibody-functionalized micromotors. Fig. 1Ac shows a functionalized micromotor completely covered by spores after navi-

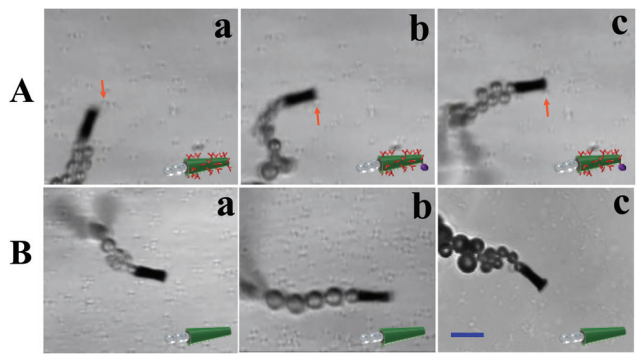

Fig. 2 Micromotors capturing and transporting *B. globigii* spores. (A) Time-lapse images (taken from ESI Video 2†) of functionalized micromotors approaching (a), contacting (b) and carrying (c) *B. globigii* spores present at 9.5 × 10^5 CFU ml^{-1} (level 1×) in the solution. (B) Negative controls: time-lapse images of unmodified micromotor contacting but not capturing the spores at 5× (a), as well as modified micromotor bypassing both *S. aureus* cells at 10× (b) and *E. coli* at 1× (c) (images from ESI Video 3†). Conditions: PBS solution pH 7.4, containing 3.75% H_2O_2 and 5% NaCh. Spores, highlighted with red arrows. Scale bar, 20 μm.

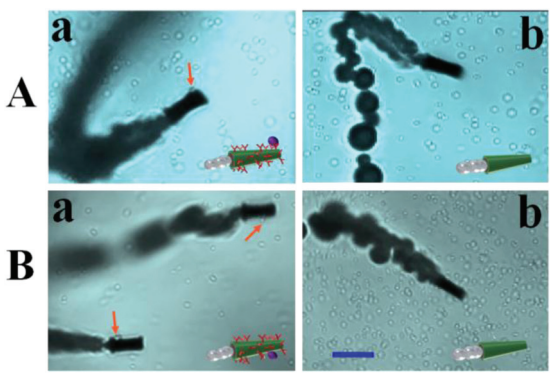

Fig. 3 Micromotors capturing and transporting *B. globigii* spores in lake and tap water samples. Time-lapse images (taken from ESI Videos 4 and 5,† respectively) showing an anti-*B. globigii* antibody-functionalized micromotors carrying *B. globigii* spores in a lake (A) and tap water (B) samples at 1× concentration (a) and unmodified micromotors bypassing the spores at 2× and even 5× excess concentrations, (Ab and Bb), respectively, as negative controls. Other conditions, as in Fig. 2. Spores are highlighted with red arrows. Scale bar, 20 μm.

gating in a contaminated solution for only 10 min. Based on the micromotor and spores geometry we estimated the micromotor-loading capacity. Assuming a truncated cone shaped micromotor with 5 and 6.7 μm of minor and major radii, respectively, and 20 μm wide (738 μm^2 surface area) and rounded spores of 1 μm radii (0.78 μm^2 area), in the best of the cases it would be possible to confine 946 spores per micromotor and the 8×10^3 micromotors used for each drop in our experiments are capable of capturing a total of 7.57×10^6 spores, which is ~40-fold more than the total population of cells used here for the testing (1.9×10^5/drop or 9.5×10^7 ml^{-1}). These results demonstrate the potential of our micromotors to preconcentrate spores at their outermost surface toward isolation (removal) and mitigation (destruction) tasks.

The next set of experiments was conducted to demonstrate the ability of unmodified micromotors to accelerate the mixing of antimicrobial agents that damage spores cell wall towards inactivation and eventual mitigation of their harm. Common antimicrobial agents, including bleach, chlorine dioxide, hydrogen peroxide, and paraformaldehyde have been shown to be effective for inactivation of bacillus spores.[3]

However, accessibility of oxidant solutions is limited when decontaminating high volumes of spore-containing solutions or where stirring is not possible, *e.g.* using microscale volumes, lab-on-a-chip formats, or hostile remote settings. To demonstrate the motor-accelerated destruction of spores, 8×10^5 micromotors were allowed to navigate in 15 ml aqueous quiescent solution containing 3.5×10^{10} *B. globigiis* spores, 1.5% H_2O_2 and 2% NaCh for up to 1 hour. The population of the damaged/intact cells was estimated at 15 min intervals by using the commercial LIVE/DEAD® *Bac*Light bacterial viability kit, which has shown to correlate well with live/dead cells assay obtained with standard plate counts. Yet, instead of harvesting cells that would allow us to know if the cells are live or dead, for practicality in this work we used the convention 'damaged/intact cells' for cells with compromised and unaltered membranes, respectively, without any additional growth testing. Syto-9 dye from the kit stained all the population of cells while propidium iodide penetrated only the damaged cells. Fig. 4 demonstrates the potential of micromotors to accelerate the damage of *B. globigii* spores. Fluorescence images of *B. globigii* spores treated with a mixture of micromotors and H_2O_2 (the latter has a dual purpose: cells oxidation and micromotor propulsion) show an increase in the population of the damaged cells with time (Fig. 4A(b–f)), compared to the total population of cells (Aa). However, no apparent increase in the damaged cells is observed in the absence of micromotors (Fig. 4B(b–f)), relative to the total cells population (Ba). These results are consistent with earlier reports for destruction of spores with bactericides.[3,17]

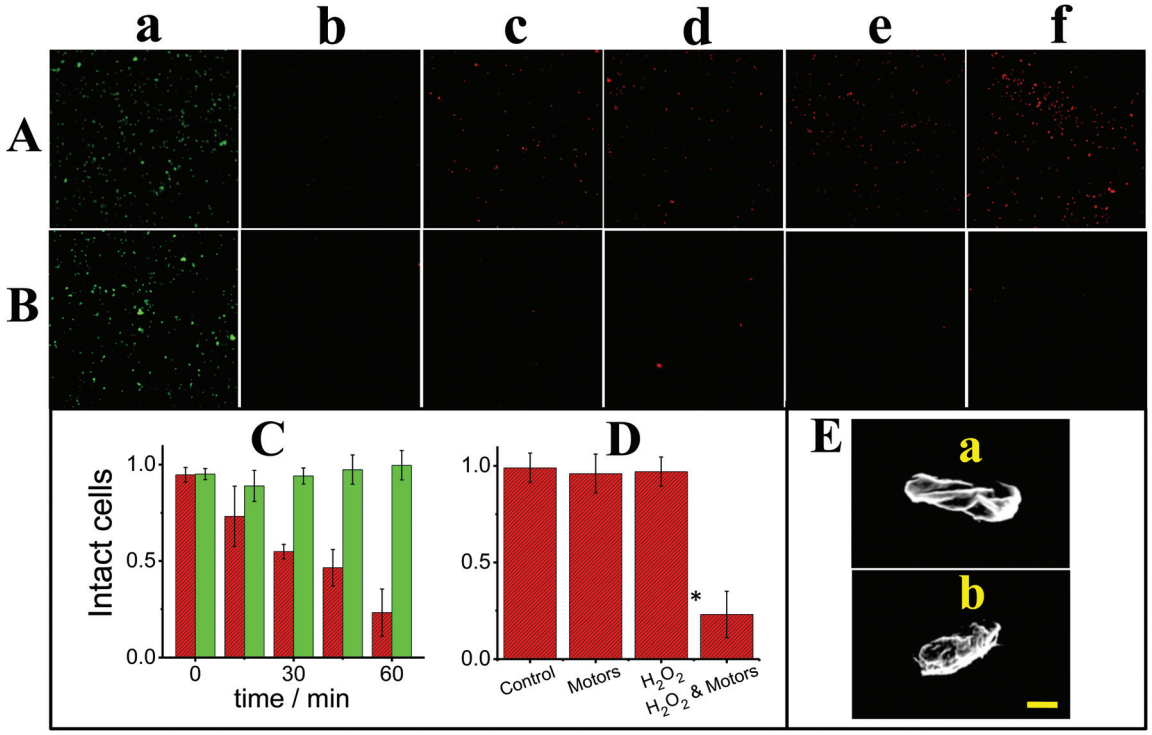

Fig. 4 Micromotors-accelerated destruction of *B. globigii* spores. Fluorescence images of damaged *B. globigii* spores after treatment with H_2O_2 and micromotors (A) or only H_2O_2 (B) for 0, 15, 30, 45 and 60 min (b–f, respectively) and total cell count (a). Time dependence of damaged spores treated with H_2O_2 and micromotors and treated only with quiescent H_2O_2 (C, lined red and green bars, respectively) and comparison respect to only H_2O_2, only motors and untreated cells (control in water) for 60 min (D), respectively (all of them relative to the cell total number); see ESI† for details. SEM Images (E) for untreated (intact) spore (a) compared to micromotors-accelerated H_2O_2 treated spore (b). Conditions: 8×10^5 micromotors navigating in 15 ml of an aqueous solution containing 3.5×10^{10} *B. globigii* cells, 1.5% H_2O_2 and 2% NaCh. Scale bar, 20 μm in B and 0.5 μm in E. Error bars represent the standard deviation of 3 counts and *statistically significant differences ($p < 0.05$).

Fig. 4C shows the time dependence of the damaged spores that were treated with micromotors-driven H_2O_2 compared to those without the micromotors. Fig. 4D illustrates the population of spores damaged by the micromotor-accelerated treatment as compared with only H_2O_2 at the same concentration (lacking micromotors), and only motors (with no H_2O_2), and the control in water after 60 min. While the micromotors-accelerated oxidizing treatment under mild conditions (1.5% H_2O_2) damaged around 77% of the cells within 60 min, treatments involving only the H_2O_2 or the motors had no statistically significant differences ($p < 0.05$), relative to the untreated control cells (in water). After 1 h treatment in the presence of these micromotors it was found that 77% of the spores are damaged and 23% spores are alive. These results indicate that none of the treatments by itself has a significant effect on the spore decontamination process and that only the H_2O_2 treatment in the presence of swimming micromotors results in a significant accelerated destruction capability. The limited access of the antimicrobial solution to the spores in the absence of micromotors (or with static motors) is dramatically accelerated when these motors are actively swimming in the spores-contaminated solution. The self-propelled micromotors are thus efficiently mixing the sporicidal solution, thereby facilitating its access to cells for their efficient destruction (damage). The SEM images of a smooth intact untreated spore, as compared to the rough shrunk treated one (Fig. 4E, a *vs.* b, respectively), are consistent with the mentioned micromotor-accelerated cells damage. These data demonstrate that micromotors are able to speed up the accessibility of oxidizing agents to the spores and to enhance the inactivation efficiency and potential destruction. Such process minimizes the need for excessive reagent levels and hence of their effects upon environmental and biological matrices.

Conclusions

We have demonstrated a micromotor-based approach capable of rapid screening, detecting, isolating and damaging biothreat agent simulant spores from nearly untreated samples in a simplified fashion. The 'on-the-fly' spore detection protocol relies on the movement of an anti-*B. globigii* antibody-functionalized micromotors in a contaminated solution to recognize, capture and transport single and multiple *B. globigii* spores. These functionalized micromotors show no interaction with excess of other bacterial counterparts. The new micromotors can concentrate multiple spores at their surface, as was successfully demonstrated using tap and lake real water samples as model habitats of the spores. Unmodified micromotors offered a built-in mixing capability and were successfully used for accelerating the mixing of mild quiescent oxidizing solutions with the concomitant acceleration of the cell damage. While the functionalized micromotors allow for a label-free visual identification of the presence and identity of the threat, the micromotor-induced mixing is shown to accelerate the immunoreactions as well as the screening and destruction processes. The new micromotor assay thus represents a useful addition to the rapidly growing arsenal of motor-based bioseparation protocols.[18] Further work would eliminate the requirement of the peroxide fuel in connection with biocompatible fuels and environmentally friendly nanomachines. This micromotor strategy will pave the way for the efficient and rapid destruction of BWA with minimal sample processing in remote field conditions where controlled mechanical agitation is impossible. The new concept can be extended to different biological threats. The new micromotor-based approach offers considerable promise for the development of effective systems that rapidly alert about the presence of a biological target and can mitigate such potential threat.

Acknowledgements

This project received support from the Defense Threat Reduction Agency–Joint Science and Technology Office for Chemical and Biological Defense (HDTRA1-13-1-0002). G. P. acknowledges financial support from the China Scholarship Council. Authors thank J. Walker from Tetracore and W. Scott Jonas from the U.S. Army-Dugway Proving Ground for providing us with the spores and V. Garcia-Gradilla and C. R. Kane for their assistance in the experiments.

Notes and references

1 (*a*) H. C. Lane, J. L. Montagne and A. S. Fauci, *Nat. Med.*, 2001, **7**, 1271–1273; (*b*) B. Durodié, *Curr. Opin. Biotechnol.*, 2004, **15**, 264–268; (*c*) N. M. Cirino, K. A. Musser and C. Egan, *Expert Rev. Mol. Diag.*, 2004, **4**, Add: Book 841–857.

2 (*a*) B. L. Mangold, J. Lynn and T. W. O'Brien, *United States Patent US007618783B2*, US 7,618,783 B2 Nov. 17, 2009; (*b*) G. W. Long and T. O'Brien, *J. Appl. Microbiol.*, 1999, **87**, 214; (*c*) A. P. Phillips, A. M. Campbell and R. Quinn, *FEMS Microbiol. Immunol.*, 1988, **1**, 169–178; (*d*) J. W. Ezzell and T. G. Abshire, *Infect. Immun.*, 1988, **56**, 349–356; (*e*) A. P. Phillips and J. W. Ezzell, *J. Appl. Bacteriol.*, 1989, **66**, 419–432.

3 (*a*) E. A. S. Whitney, M. E. Beatty, T. H. Taylor, R. Weyant, J. Sobel, M. J. Arduion and D. A. Ashford, *Emerging Infect. Dis.*, 2003, **9**, 623–627; (*b*) G. Wagner and Y. C. Yang, *Ind. Eng. Chem. Res.*, 2002, **41**, 1925–1928; (*c*) Q. Li, S. Mahendra, D. Y. Lyon, L. Brunet, M. V. Liga, D. Li and P. J. J. Alvarez, *Water Res.*, 2008, **42**, 4591–4602; (*d*) M. Lilly, X. Dong, E. McCoy and L. Yang, *Environ. Sci. Technol.*, 2012, **46**, 13417–13424.

4 Y. F. Mei, G. S. Huang, A. A. Solovev, E. B. Urena, I. Monch, F. Ding, T. Reindl, R. K. Y. Fu, P. K. Chu and O. G. Schmidt, *Adv. Mater.*, 2008, **20**, 4085–4090.

5 W. Gao, S. Sattayasamitsathit, J. Orozco and J. Wang, *J. Am. Chem. Soc.*, 2011, **133**, 11862–11864.

6 G. Zhao and M. Pumera, *RSC Adv.*, 2013, **3**, 3963–3966.

7 J. Wang, *Nanomachines: Fundamentals and Applications*, John Wiley & Sons, Weinheim, 2013.
8 (*a*) J. Wang and W. Gao, *ACS Nano*, 2012, **6**, 5745–5751; (*b*) S. Campuzano, J. Orozco, D. Kagan, M. Guix, W. Gao, S. Sattayasamitsathit, J. C. Claussen, A. Merkoci and J. Wang, *Nano Lett.*, 2012, **12**, 396–401; (*c*) J. Orozco, S. Campuzano, D. Kagan, M. Zhou, W. Gao and J. Wang, *Anal. Chem.*, 2011, **83**, 7962–7969; (*d*) M. García, J. Orozco, M. Guix, W. Gao, S. Sattayasamitsathit, A. Escarpa, A. Merkoçi and J. Wang, *Nanoscale*, 2013, **5**, 1325–1331.
9 E. Morales-Narváez, M. Guix, M. Medina-Sánchez, C. Mayorga-Martinez and A. Merkoçi, *Small*, 2014, **10**, 2542–2548.
10 X. Yu, Y. Li, J. Wu and H. Ju, *Anal. Chem.*, 2014, **86**, 4501–4507.
11 A. A. Solovev, W. Xi, D. H. Gracias, S. M. Harazim, C. Deneke, S. Sanchez and O. G. Schmidt, *ACS Nano*, 2012, **6**, 1751–1756.
12 (*a*) W. Gao and J. Wang, *ACS Nano*, 2014, **8**, 3170–3180; (*b*) L. Soler and S. Sanchez, *Nanoscale*, 2014, **6**, 7175–7182.
13 J. Orozco, G. Cheng, D. Vilela, S. Sattayasamitsathit, R. Vazquez-Duhalt, G. Valdes-Ramirez, O. S. Pak, A. Escarpa, C. Kan and J. Wang, *Angew. Chem., Int. Ed.*, 2013, **52**, 13276–13279.
14 L. Soler, V. Magdanz, V. M. Fomin, S. Sanchez and O. G. Schmidt, *ACS Nano*, 2013, **7**, 9611–9620.
15 Ö. Türkarslan, S. K. Kayahan and L. Toppare, *J. Solid State Electrochem.*, 2009, **13**, 657–663.
16 (*a*) C. Supaporn, A. Kradtap, K. T. Wijayawardhana, H. Schlueter, B. Halsall and W. R. Heineman, *Anal. Chim. Acta*, 2001, **444**, 13–26; (*b*) S. P. Mulvaney, K. M. Myers, P. E. Sheehan and L. J. Whitman, *Biosens. Bioelectron.*, 2009, **24**, 1109–1115.
17 (*a*) C. A. Loshon, E. Melly, B. Setlow and P. Setlow, *J. Appl. Microbiol.*, 2001, **91**, 1051–1058; (*b*) P. C. Genest, B. Setlow, E. Melly and P. Setlow, *Microbiology*, 2002, **148**, 307–314; (*c*) T. Murray, L. David, C. Popham, B. Pearson, A. R. Hand and P. Setlow, *J. Bacteriol.*, 1998, **180**, 6493–6502.
18 (*a*) S. Campuzano, D. Kagan, J. Orozco and J. Wang, *Analyst*, 2012, **136**, 4621–4630; (*b*) L. Restrepo-Perez, L. Soler, C. S. Martínez-Cisneros, S. Sanchez and O. Schmidt, *Lab Chip*, 2014, **14**, 2914–2917.